

# Robot Location Using Single Views of Rectangular Shapes

Royal Lee

Institute of System Engineering, Chung Cheng Institute of Technology, Taoyuang, Taiwan 33508, Republic of China

Po-Chiang Lu

Department of Electrical Engineering, Chung Cheng Institute of Technology, Taoyuang, Taiwan 33508, Republic of China

Wen-Hsiang Tsai

Department of Computer and Information Science, National Chiao Tung University, Hsinchu, Taiwan 30050, Republic of China

**ABSTRACT:** In man-made environments, rectangular shapes can be seen almost everywhere. It is thus convenient to use rectangular shapes for robot location, which is equivalent to the problem of close-range space resection encountered in photogrammetric engineering. A new method for robot location using mutually parallel or perpendicular line pairs in observed rectangular shape images is proposed. From a monocular image of any object with at least a rectangular shape, image processing and numerical analysis techniques are applied to extract the projection characteristics of each corner point in the rectangular shape. The position and orientation parameters of a camera mounted on the robot can then be computed for robot location. Multiple rectangular shapes can be utilized to promote the accuracy of the parameters. Partial rectangular shapes also can be utilized. A major merit of the method is that the solution can be uniquely and analytically determined without iterative computation. Experimental results show the feasibility of the proposed approach. Error analysis useful for determining location precision is also included.

## INTRODUCTION

FOR A ROBOT TO NAVIGATE in a building environment such as in a house or along a corridor, an important task is to locate the position of the robot with respect to known objects. This type of so-called robot location problem is actually equivalent to the problem of close-range space resection encountered in photogrammetric engineering.

One approach to this problem is to use the stereo disparity principle to get three-dimensional (3-D) information. The correspondence of two images involved in this approach in general is difficult and time-consuming. Numerical analysis with iterative steps is usually necessary, which is also computationally expensive.

Locating robot positions using monocular images is another approach which is generally more efficient. Fukui (1981) described an algorithm for determining the position of a robot from a single TV image of a specific diamond-shaped mark set on a wall. A constraint of the approach is that the lens center of the TV camera must be located at the same height as the diamond center.

Courtney and Aggarwal (1984) proposed an extension of the 2-D technique proposed by Fukui. The restriction on keeping the camera at the level of the mark center is relaxed. In order to solve an underdetermined system of two equations with three unknown, two methods are proposed. One is to add another mark, and the other is to assume that the height of the camera relative to the mark is known.

Magee and Aggarwal (1984) proposed a method for determining robot positions uniquely by viewing a single sphere with horizontal and vertical great circles and computing the distance, the elevation, and the azimuth angles of the camera with respect to the sphere.

Haralick and Chu (1984) described the use of parametric planar or nonplanar curves to determine camera parameters. Camera angle parameters are solved first. The camera position parameters under these angles are computed next. An optimization technique is employed to solve nonlinear equations for the former problem. The number of curve points involved in the iterative computation usually is large.

Chou and Tsai (1986) used Y-shaped house corners as the standard mark to locate robot positions. It is assumed that the distance from the camera to the room ceiling is known. A Y-shaped corner is composed of three perpendicular planes, or alternatively, of three perpendicular lines with each line being the intersection of a pair of planes. Analytic solutions can be derived.

Ethrog (1984) proposed a method for determining the tilt angles and the nine interior orientation parameters (including the radial lens distortion) of a non-metric film-camera using the parallel and perpendicular lines of the photographed objects instead of the control points.

Tseng *et al.* (1987) proposed an approach to determining the 3-D position of a mobile robot using the information of the vanishing points of the 2-D perspective projection of a cube. The locations of the vanishing points are iteratively modified to satisfy the facts that the length of the cube is known and that the edges of the cube are mutually perpendicular.

El-Hakim (1984) proposed a vision system consisting of a single camera, a projector, and a digital image processing unit. The object coordinates of any point on the projected line can be determined from the image coordinates obtained from the digital image processor and from the known location of the line in the projector system, provided that the relative positions and orientations of the camera and the projector are known.

Tommaselli and Lugini (1988) proposed a mathematical model in order to establish a functional relationship between the straight features in an object and in the image space, without the necessity of point-to-point correspondence. This model is based on the equivalence between the definition parameters from the plane determined by each straight feature and the camera lens center, so that it can be applied to the resection and the analytical stereo model formation problems.

The approach proposed in this paper makes use of rectangular shapes which are very common in human environments. Examples of objects containing rectangular shapes include doors, windows, walls, table surfaces, announcement boards, box sides, corridor scenes, etc. This makes the approach more convenient and practical for general applications because no extra objects or shapes need be created and placed for robot location.

The goal of robot location, as defined in this study, is to provide robot position information with respect to available rectangular shapes along the navigation path of a mobile robot so that the robot can follow the predetermined path in a collision-free manner. By assuming that the width of the path at any spot is large enough, it is reasonable to allow a small error percentage, say 5 percent, in computed robot positions with respect to the path widths. Because each of the robot location tasks along the navigation path is independent, the error essentially is not additive. And so, collision-free navigation can be achieved although small location errors might cause the robot to navigate along curves instead of straight lines within the path.

Some merits of the proposed approach are as follows:

- Single views of known rectangular shapes are sufficient for robot location; binocular image pairs are not necessary.
- The corner points and the lines through the corners can be detected automatically using digital image processing and numerical analysis techniques.
- Partial rectangular shapes can also be utilized as long as two points and three line segments are available.
- Location accuracy can be improved if multiple rectangular shapes are observed, provided that the relative positions and orientations of each rectangular shape are known in advance.
- Analytic algebraic formulae can be utilized in the solution. No complicated trigonometric function is involved. This saves a lot of computation time.

The location formulae are derived in the next section. Computation of camera parameters from partial or multiple rectangular shape image is then described. Experimental results and error analysis are included, followed by conclusions and suggestions for further research.

**ROBOT LOCATION BY COMPLETE RECTANGULAR SHAPES**

Collinearity specifies the condition that the camera lens center C, any object point A, and the image a of A all lie along a straight line. The collinearity condition is illustrated in Figure 1, where xyz is a tilted camera coordinate system, x'y'z' is the transformed camera system which is parallel to the XYZ space coordinate system, (x', y', z') are the transformed image coordinates of the measured image coordinates (x<sub>a</sub>, y<sub>a</sub>) of a, and (X<sub>C</sub>, Y<sub>C</sub>, Z<sub>C</sub>) and (X<sub>A</sub>, Y<sub>A</sub>, Z<sub>A</sub>) are respectively the coordinates of C and A in the space coordinate system XYZ. In this section, we want to derive the camera location parameters, including the position parameters X<sub>C</sub>, Y<sub>C</sub>, and Z<sub>C</sub>, and the orientation parameters ψ, θ, and δ (the pan, tilt, and swing angles of the camera), in terms of the image coordinates of the corner points of the rectangular shapes. The orientation parameters are solved first and the position parameters are computed accordingly.

**DERIVATION OF THE CAMERA ORIENTATION PARAMETERS**

The points P, Q, R, and S in Figure 2 lie on a rectangle in the object space. The line segment PS and the line segment QR are parallel to the X-axis in the object space and all the points on PS or QR have the same Y and Z coordinates. The space coordinate system is oriented in such a way that all of its axes are parallel to the sides of the rectangle. Using the law of collinearity (Ackermann, 1976; Wolf, 1974) and the fact that Y<sub>1</sub> = Y<sub>4</sub> and Z<sub>1</sub> = Z<sub>4</sub>, it is easy to derive

$$\frac{Y_1 - Y_C}{Z_1 - Z_C} = \frac{r_{21}x_1 + r_{22}y_1 - r_{23}f}{r_{31}x_1 + r_{32}y_1 - r_{33}f} = \frac{Y_4 - Y_C}{Z_4 - Z_C} = \frac{r_{21}x_4 + r_{22}y_4 - r_{23}f}{r_{31}x_4 + r_{32}y_4 - r_{33}f} \quad (1)$$

where (x<sub>1</sub>, y<sub>1</sub>) and (x<sub>4</sub>, y<sub>4</sub>) are the image coordinates of space points P and S, respectively; the orthogonal orientation matrix elements r<sub>ij</sub> are functions of the rotation angles (pan, tilt, and swing); and f is the camera focal length. Here, the coordinates

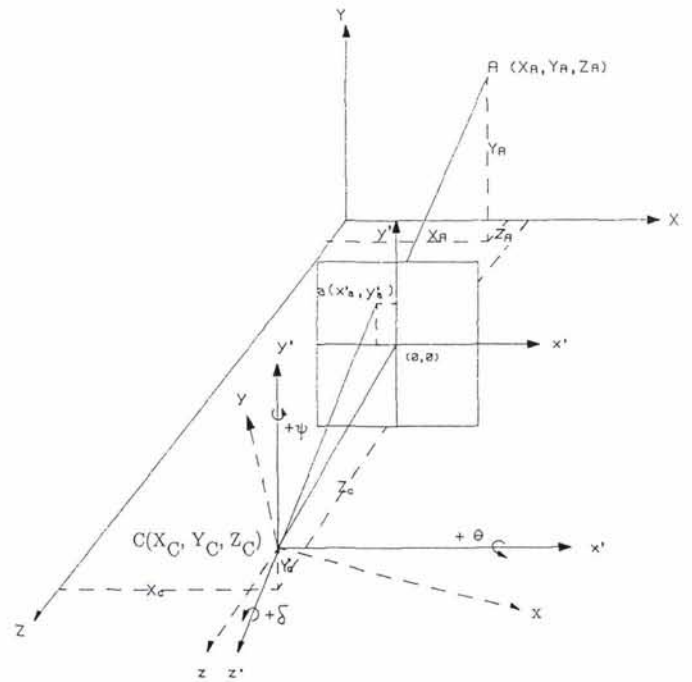


FIG. 1. The relationship between the global coordinate system and the camera coordinate system.

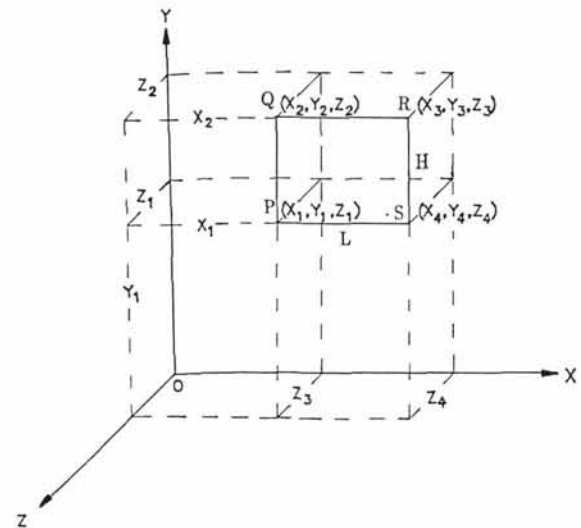


FIG. 2. A rectangle PQRS in the object space which has PQ and RS parallel to the Y axis and PS and QR parallel to the X axis.

of the image center are assumed to be zeroes. Equation (1) can be rewritten as

$$\begin{aligned} & (r_{22}r_{33} - r_{23}r_{32})(y_1 - y_4)f \\ & + (r_{23}r_{31} - r_{21}r_{33})(x_4 - x_1)f \\ & + (r_{21}r_{32} - r_{22}r_{31})(y_1x_4 - x_1y_4) = 0. \end{aligned} \quad (2)$$

But the elements r<sub>ij</sub> must fulfill the following conditions:

$$\begin{aligned} r_{22}r_{33} - r_{23}r_{32} &= r_{11}, \\ r_{23}r_{31} - r_{21}r_{33} &= r_{12}, \\ r_{21}r_{32} - r_{22}r_{31} &= r_{13}. \end{aligned} \quad (3)$$

and so we obtain from Equations 2 and 3 the following linear equation:

$$r_{11}(y_1 - y_4)f + r_{12}(x_4 - x_1)f + r_{13}(y_1x_4 - x_1y_4) = 0. \quad (4)$$

In a similar way using the image coordinates  $(x_2, y_2)$  and  $(x_3, y_3)$  of space points Q and R, respectively, we obtain

$$r_{11}(y_2 - y_3)f + r_{12}(x_3 - x_2)f + r_{13}(y_2x_3 - x_2y_3) = 0. \quad (5)$$

From Equations 4 and 5 and the condition

$$r_{11}^2 + r_{12}^2 + r_{13}^2 = 1,$$

we obtain

$$r_{11} = E_1 r_{13}, r_{12} = D_1 r_{13}, r_{13} = \pm (1 + D_1^2 + E_1^2)^{-1/2}, \quad (6)$$

where

$$D_1 = \frac{(y_2 - y_3)(y_1x_4 - x_1y_4) - (y_1 - y_4)(y_2x_3 - x_2y_3)}{(y_1 - y_4)(x_3 - x_2)f - (y_2 - y_3)(x_4 - x_1)f},$$

$$E_1 = -[D_1(x_4 - x_1)f + (y_1x_4 - x_1y_4)]/(y_1 - y_4)f.$$

The sign of the square root value  $r_{13}$  has to be determined. If we can constrain the camera angles to be less than  $90^\circ$  and the camera position to lie in a certain quadrant, the sign of  $r_{13}$  can be determined by the direction of the pan angle  $\psi$ ; if the pan angle  $\psi$  is rotated counterclockwise, then the sign is positive. The direction of the pan angle can be detected by the perspective distortion of the rectangular shape (Ackermann, 1976; Wolf, 1974) and the known 3-D position of the shape. In a similar way, using the line segments  $\overline{PQ}$  and  $\overline{RS}$  which are parallel to the Y-axis in the object space, we obtain

$$r_{21}(y_1 - y_2)f + r_{22}(x_2 - x_1)f + r_{23}(y_1x_2 - x_1y_2) = 0, \quad (7)$$

$$r_{21}(y_3 - y_4)f + r_{22}(x_4 - x_3)f + r_{23}(y_3x_4 - x_3y_4) = 0, \quad (8)$$

$$r_{21}^2 + r_{22}^2 + r_{23}^2 = 1. \quad (9)$$

From Equations 7, 8, and 9,  $r_{21}$ ,  $r_{22}$ , and  $r_{23}$  can be solved as follows:

$$r_{21} = E_2 r_{23}, r_{22} = D_2 r_{23}, r_{23} = \pm (1 + D_2^2 + E_2^2)^{-1/2}, \quad (10)$$

where

$$D_2 = \frac{(y_3 - y_4)(y_1x_2 - x_1y_2) - (y_1 - y_2)(y_3x_4 - x_3y_4)}{(y_1 - y_2)(x_4 - x_3)f - (y_3 - y_4)(x_2 - x_1)f},$$

$$E_2 = -[D_2(x_2 - x_1)f + (y_1x_2 - x_1y_2)]/(y_1 - y_2)f.$$

The sign of  $r_{23}$  can be determined by the direction of the tilt angle  $\theta$ . Because the term  $\cos\psi$  is always positive, if the tilt angle  $\theta$  is rotated counterclockwise, then the sign is positive. The direction of the tilt angle can be detected by the perspective distortion of the rectangular shape and the known 3-D position of the shape.

From the relation of the orthogonal orientation matrix elements, we obtain the remaining three matrix elements as follows:

$$\begin{aligned} r_{31} &= r_{12}r_{23} - r_{13}r_{22} \\ r_{32} &= r_{21}r_{13} - r_{11}r_{23} \\ r_{33} &= r_{11}r_{22} - r_{12}r_{21} \end{aligned} \quad (11)$$

At this point, the nine orientation elements  $r_{ij}$  have all been solved (Equations 6, 10, and 11). The orientation angles can

then be solved (Ackermann, 1976; Wolf, 1974) using the equations

$$\psi = \sin^{-1}(r_{13}), \quad (12)$$

$$\theta = \tan^{-1}(-r_{23}/r_{33}), \quad (13)$$

$$\delta = \tan^{-1}(-r_{12}/r_{11}). \quad (14)$$

#### DERIVATION OF THE CAMERA POSITION PARAMETERS

In Figure 2, we assume that the side lengths  $L$  and  $H$  of the rectangle are known. The length  $L$ , which is the distance between point Q and point R or between point P and point S, can be rewritten as

$$L = X_3 - X_2 = (X_3 - X_C) - (X_2 - X_C)$$

where  $X_C$  is the X coordinate of the camera lens center C. Dividing the above equation by the term  $(Z_0 - Z_C)$  with  $Z_0 = Z_2 = Z_3$  and using the law of collinearity, we obtain

$$\begin{aligned} \frac{L}{Z_0 - Z_C} &= \frac{X_3 - X_C}{Z_3 - Z_C} - \frac{X_2 - X_C}{Z_2 - Z_C} \\ &= \frac{r_{11}x_2 + r_{12}y_2 - r_{13}f}{r_{13}x_3 + r_{12}y_3 - r_{13}f} - \frac{r_{11}x_3 + r_{12}y_3 - r_{13}f}{r_{31}x_2 + r_{32}y_2 - r_{33}f} \\ &= C_1 - C_2 \end{aligned} \quad (15)$$

where  $C_1$  and  $C_2$  are known values representing the two terms on the right-hand side of Equation 15 which include the known values  $r_{ij}$ ,  $(x_3, y_3)$ ,  $(x_2, y_2)$ , and  $f$ . From Equation 15 we obtain

$$Z_C = Z_0 - \frac{L}{C_1 - C_2}, \quad (16)$$

$$X_C = X_3 - C_1(Z_0 - Z_C),$$

or

$$X_C = X_2 - C_2(Z_0 - Z_C). \quad (17)$$

Using the law of collinearity again, we obtain

$$\frac{Y_2 - Y_C}{Z_2 - Z_C} = \frac{r_{21}x_2 + r_{22}y_2 - r_{23}f}{r_{31}x_2 + r_{32}y_2 - r_{33}f} = C_3, \quad (18)$$

$$\frac{Y_3 - Y_C}{Z_3 - Z_C} = \frac{r_{21}x_3 + r_{22}y_3 - r_{23}f}{r_{13}x_3 + r_{12}y_3 - r_{13}f} = C_4 \quad (19)$$

where  $C_3$  and  $C_4$  are known values. From Equations 18 and 19 we obtain

$$Y_C = Y_2 - C_3(Z_0 - Z_C),$$

$$Y_C = Y_3 - C_4(Z_0 - Z_C). \quad (20)$$

Up to now we have derived the formulae for all the position parameters  $(X_C, Y_C, Z_C)$  (Equations 16, 17, and 20). From the side length  $H$ , we can derive in a similar way another set of formulae for the position parameters. Because each side length of the rectangle can be used to decide one set of camera position parameters  $X_C$ ,  $Y_C$ , and  $Z_C$ , the four side lengths can be used to construct four sets of parameters. A simple way to utilize all the four sets of data is to take the average of the data as the final location result. In case all computations of a parameter are not of equal accuracy due to view angles, weighted averaging instead may be adopted with smaller weights being assigned to the data which are less accurate (e.g., with larger standard deviations in a sequence of experimental observations). This completes the derivation of the camera location parameters  $X_C$ ,  $Y_C$ ,  $Z_C$ ,  $\psi$ ,  $\theta$ , and  $\delta$ . Note that all the six parameters can be computed by closed-form algebraic formulae. No iterative computation is required. This improves the computation speed

and makes the proposed approach more practical for real applications. This is one of the merits of the proposed approach.

**ROBOT LOCATION USING PARTIAL AND MULTIPLE RECTANGULAR SHAPES**

In certain cases, a rectangular shape may be seen only partially. It was found in this study that partial rectangular shapes are also useful for robot location. To solve the problem of using partial rectangular images, we propose another method for finding the camera parameters.

**THE USE OF A PARTIAL SHAPE WITH THREE CORNER POINTS**

In the image of a partial rectangular shape as shown in Figure 3, the corner point *s* cannot be seen. Let the equation of the image of line *L*<sub>3</sub> through corner point *R*(*X*<sub>3</sub>, *Y*<sub>3</sub>, *Z*<sub>3</sub>) be described by

$$x_p + b_3 y_p + c_3 = 0 \tag{21}$$

where *x*<sub>*p*</sub>, *y*<sub>*p*</sub> are the image coordinates of the projection of any point on *L*<sub>3</sub> on the image plane. Because *L*<sub>3</sub> goes through object point *R*(*X*<sub>3</sub>, *Y*<sub>3</sub>, *Z*<sub>3</sub>) and is parallel to the *Y* axis, (*X*<sub>3</sub>, *Y*, *Z*<sub>3</sub>) are the space coordinates of any point on *L*<sub>3</sub> where *Y* is a free variable. Therefore, we can obtain the following equations from the law of the collinearity:

$$x_p = -f \left[ \frac{r_{11}(X_3 - X_c) + r_{21}(Y - Y_c) + r_{31}(Z_3 - Z_c)}{r_{13}(X_3 - X_c) + r_{23}(Y - Y_c) + r_{33}(Z_3 - Z_c)} \right] \tag{22}$$

$$y_p = -f \left[ \frac{r_{12}(X_3 - X_c) + r_{22}(Y - Y_c) + r_{32}(Z_3 - Z_c)}{r_{13}(X_3 - X_c) + r_{23}(Y - Y_c) + r_{33}(Z_3 - Z_c)} \right] \tag{23}$$

By eliminating the (*Y* - *Y*<sub>*c*</sub>) terms, the above equations can be reduced to

$$\begin{aligned} &x_p[(X_3 - X_c)r_{31} - (Z_3 - Z_c)r_{11}] \\ &+ y_p[(X_3 - X_c)r_{32} - (Z_3 - Z_c)r_{12}] \\ &+ f[(Z_3 - Z_c)r_{13} - (X_3 - X_c)r_{33}] = 0. \end{aligned} \tag{24}$$

Equation 24 above can be transformed into the form of Equation 21: i.e.,

$$x_p + b_3 y_p + c_3 = 0,$$

so that

$$b_3 = \frac{(X_3 - X_c)r_{32} - (Z_3 - Z_c)r_{12}}{(X_3 - X_c)r_{31} - (Z_3 - Z_c)r_{11}} \tag{25}$$

$$c_3 = \frac{f[(Z_3 - Z_c)r_{13} - (X_3 - X_c)r_{33}]}{(X_3 - X_c)r_{31} - (Z_3 - Z_c)r_{11}} \tag{26}$$

where *b*<sub>3</sub> and *c*<sub>3</sub> are the parameters of the image of line *L*<sub>3</sub> which can be measured by image processing (Chou and Tsai, 1986). From Equations 25 and 26 we obtain

$$\frac{X_3 - X_c}{Z_3 - Z_c} = \frac{b_3 r_{11} - r_{12}}{b_3 r_{31} - r_{32}} = \frac{c_3 r_{11} + r_{13} f}{c_3 r_{31} + f r_{33}} \tag{27}$$

We can eliminate the *X*<sub>*c*</sub> and the *Z*<sub>*c*</sub> terms and get

$$f(r_{32}r_{13} - r_{12}r_{33}) + b_3 f(r_{11}r_{33} - r_{13}r_{31}) - c_3(r_{31}r_{12} - r_{11}r_{32}) = 0,$$

which can be reduced to

$$r_{21}f + r_{22}b_3f - r_{23}c_3 = 0, \tag{28}$$

according to the following relations of the orthogonal rotation matrix elements:

$$\begin{aligned} r_{21} &= r_{32}r_{13} - r_{12}r_{33} \\ r_{22} &= r_{11}r_{33} - r_{13}r_{31} \\ r_{23} &= r_{31}r_{12} - r_{11}r_{32} \end{aligned}$$

Now, Equation 28 can be used to replace Equation 8. From Equations 7, 28, and 9, *r*<sub>21</sub>, *r*<sub>22</sub> and *r*<sub>23</sub> can be solved. Using the condition that line segment *QR* or *L*<sub>1</sub> is parallel to the *X* axis,

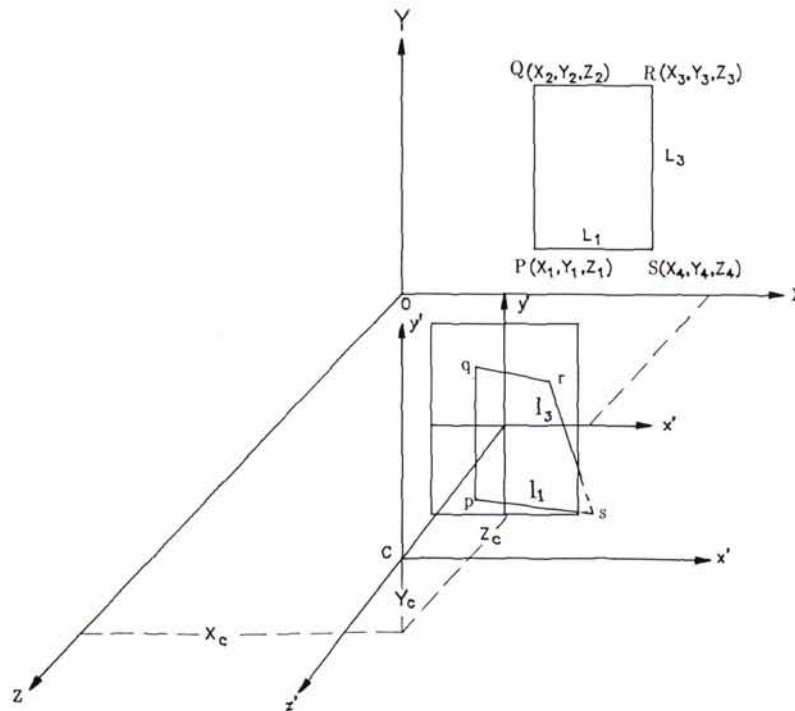


FIG. 3. A partial shape with one corner point (the image point *s*) invisible.

we can get an equation similar to Equation 28 as follows:

$$r_{11}f + r_{12}b_1f - r_{13}c_1 = 0 \quad (29)$$

with

$$b_1 = \frac{(Y_1 - Y_C)r_{32} - (Z_1 - Z_C)r_{22}}{(Y_1 - Y_C)r_{31} - (Z_1 - Z_C)r_{21}}$$

$$c_1 = \frac{f[(Z_1 - Z_C)r_{23} - (Y_1 - Y_C)r_{33}]}{(Y_1 - Y_C)r_{31} - (Z_1 - Z_C)r_{21}}$$

where  $b_1$  and  $c_1$  are the parameters of the image of line  $L_1$ , which can be measured by image processing. Equation 29 can be used to replace Equation 4. From Equations 29, 5, and 6, the elements  $r_{11}$ ,  $r_{12}$ , and  $r_{13}$  can also be solved. From the relations of the elements of the orthogonal orientation matrix, we can obtain the remaining three elements  $r_{31}$ ,  $r_{32}$ , and  $r_{33}$  by Equations 11. Using the nine orientation elements and the lengths of line segments  $\overline{PQ}$  and  $\overline{QR}$ , we can obtain, in a way similar to that complete rectangular shapes, the angle parameters  $\psi$ ,  $\theta$ , and  $\delta$  and the position parameters  $X_C$ ,  $Y_C$ , and  $Z_C$ .

THE USE OF A PARTIAL SHAPE WITH TWO CORNER POINTS

In the image of a partial rectangular shape as shown in Figure 4, corner points  $P$  and  $S$  cannot be seen. Lines  $L_2$  and  $L_3$  go respectively through object points  $Q(X_2, Y_2, Z_2)$  and  $R(X_3, Y_3, Z_3)$  and are parallel to the  $Y$  axis. The image of the two lines can be described by the equations

$$x_p + b_i y_p + c_i = 0, \quad i=2, \text{ and } 3. \quad (30)$$

In a similar way to that for a partial shape with three corner points, we can obtain two equations as follows:

$$r_{21}f + r_{22}b_2f - r_{23}c_2 = 0, \quad (31)$$

$$r_{21}f + r_{22}b_3f - r_{23}c_3 = 0 \quad (32)$$

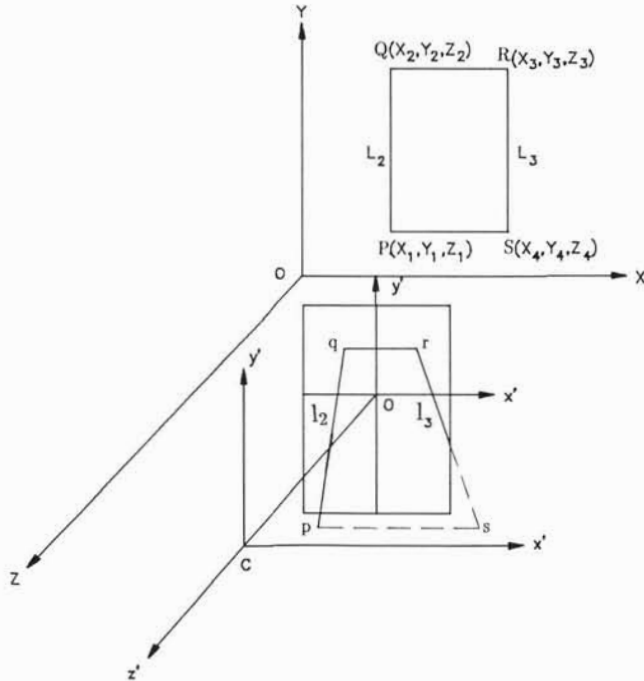


FIG. 4. A partial shape with two corner points (the image points  $p$  and  $s$ ) invisible.

where

$$b_2 = \frac{(X_2 - X_C)r_{32} - (Z_2 - Z_C)r_{12}}{(X_2 - X_C)r_{31} - (Z_2 - Z_C)r_{11}}$$

$$c_2 = \frac{f[(Z_2 - Z_C)r_{13} - (X_2 - X_C)r_{33}]}{(X_2 - X_C)r_{31} - (Z_2 - Z_C)r_{11}}$$

$$b_3 = \frac{(X_3 - X_C)r_{32} - (Z_3 - Z_C)r_{12}}{(X_3 - X_C)r_{31} - (Z_3 - Z_C)r_{11}}$$

$$c_3 = \frac{f[(Z_3 - Z_C)r_{13} - (X_3 - X_C)r_{33}]}{(X_3 - X_C)r_{31} - (Z_3 - Z_C)r_{11}}$$

The values of  $r_{21}$ ,  $r_{22}$ , and  $r_{23}$  can be solved from Equations 31, 32, and 9. From the relations of the orthogonal rotation matrix elements, we know that

$$r_{11}r_{21} + r_{12}r_{22} + r_{13}r_{23} = 0, \quad (33)$$

$$r_{11}^2 + r_{12}^2 + r_{13}^2 = 1. \quad (34)$$

Because line segment  $\overline{QR}$  is parallel to the  $X$  axis, in a way similar to the derivation of Equation 4 we can obtain

$$r_{11}(y_1 - y_2)f + r_{12}(x_2 - x_1)f + r_{13}(y_1x_2 - x_1y_2) = 0. \quad (35)$$

The elements  $r_{11}$ ,  $r_{12}$ , and  $r_{13}$  can be determined using Equations 33 through 35. According to Equation 11,  $r_{31}$ ,  $r_{32}$ , and  $r_{33}$  can also be determined. In this way, we have solved all the nine elements of the rotation matrix. In a way similar to that for complete rectangular shapes, we can obtain camera position parameters using the nine orientation elements and the length of line segment  $\overline{QR}$ . Only one set of location parameters can be obtained in this case.

THE USE OF MULTIPLE RECTANGULAR SHAPES

To increase the accuracy of robot location, we would like to compute more sets of camera parameters if more rectangular shapes can be obtained, provided that the relative positions and orientations of available rectangular shapes are known in advance. This is possible, using a cube like the one shown in Figure 5. Each view of a cube provides three rectangular planes: the left, the right, and the top ones. Each plane is perpendicular to the

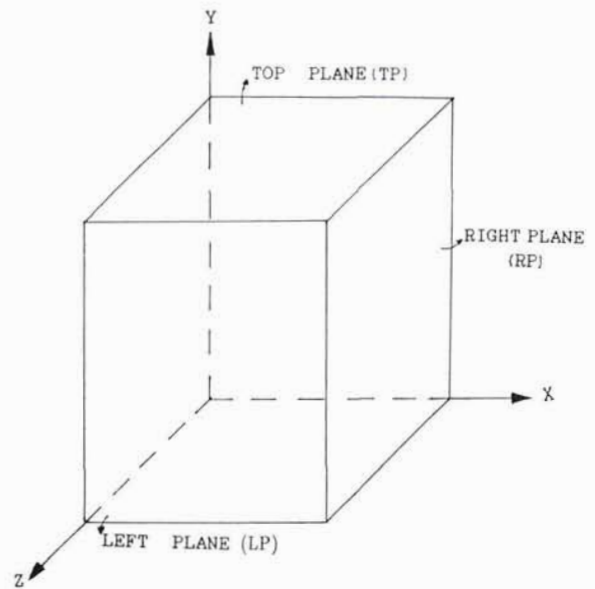


FIG. 5. A cube with multiple rectangular planes.

other two. For instance, the right plane is perpendicular to the X-Z and Y-Z planes, and is parallel to the X-Y plane. More sets of location parameters can be obtained by the use of multiple planes. The weighted average of the solution sets offers higher location accuracy.

#### EXPERIMENTAL RESULTS AND ERROR ANALYSIS

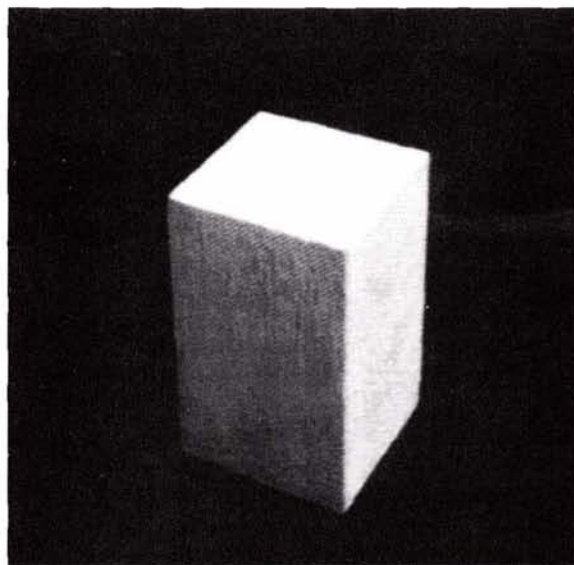
Experiments have been performed on a system including a PC-EYE (640 by 400) imaging board and a PULNIX TM-540 CCD camera equipped with 16-mm lenses for taking pictures (with a resolution of 640 by 400 by 4 bits), and a Sun workstation for image processing and location computation. The C language was used for programming. The object used in the experiments was a wood cube which includes multiple rectangular shapes.

Image and numerical analysis techniques were used for finding accurate corner coordinates and line parameters. Rectangular shapes in object images were detected by edge detection, smoothing, and thinning. Sobel edge magnitudes larger than a threshold value were detected as edge points. Eight-neighbor-averaging is applied to the edge value map in order to smooth out noise and to avoid hole creation during thinning. A fast thinning algorithm (Chen and Hsu, 1985) is adopted. It can reduce possible distortions on crossing points and branch points.

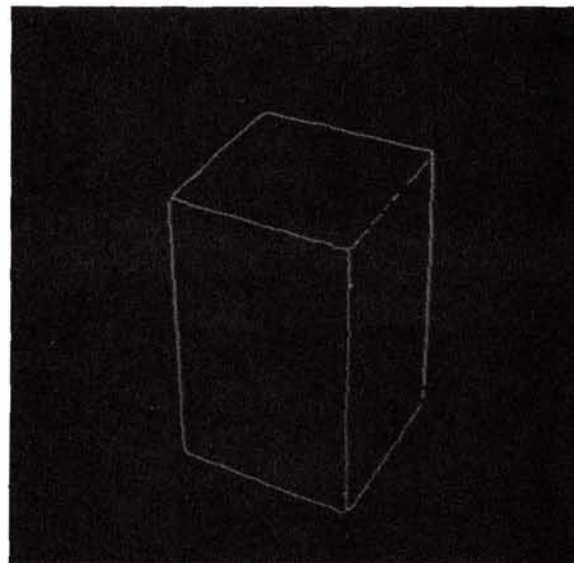
To detect the rectangular shapes, the Hough transform (Duda and Hart, 1972) is applied. The advantage of using the Hough transform in line detection is that it can endure noise and gaps to a certain limit. Examples of cube images and corresponding preprocessing results are shown in Figure 6. To get an accurate camera location, calibration for computing uniform scales of  $x$  and  $y$  image coordinates, the image center, and the camera focal length must be done first. The calibration procedures were adopted from those in Chen and Tsai (1987). Imaging distortion correction was not necessary because such distortions were found negligible for this type of application (Chen and Tsai, 1987) in a CCD camera picture.

The cube with size 70 mm by 70 mm by 100 mm was imaged eight times for testing. The space coordinates of the cube corners were determined with a standard deviation of 0.4 mm in the X and Y directions and 0.55 mm in the Z direction. The camera was used to take the images of the cube from a distance of 587 mm. Each pixel size in the image array was measured to be of the size of  $13.3 \mu\text{m}$  by  $13.4 \mu\text{m}$ . All the final location parameters are included in Table 1, in which the column "TP", "RP", "LP", and "PRP" specify the single top, right, left, and partial right plane of the cube, respectively; the row "M" specifies the reference values of the location parameters which are derived from the weighted average location parameters of the multiple planes (the top, right, and left planes) of the cube; the row "m" specifies the computed mean location parameters; the row "v" specifies the difference between the mean and the reference; the row "e" specifies the error percentage which is defined as the ratio of the deviation value of the computed position value from the reference value to the reference value; and the row " $\sigma$ " specifies the standard deviation of the eight location parameters. The symbols "L" and "S" specify the largest and the smallest error percentage, respectively. The average error percentage can be computed to be less than 5 percent. This shows the feasibility of the proposed approach for mobile robot navigation, as discussed in the introduction.

Computer simulation has additionally been performed to analyze the magnitude of the relative errors introduced by the uncertainties in the collinearity and the equation coefficients of the corner lines which are computed by image and numerical analysis techniques. Error analysis was performed 100 times with 100 different sets of artificial rectangular images created by introducing distinct Gaussian random errors. The standard de-



(a)



(b)

FIG. 6. A cube used in the experiments. (a) An image of the cube. (b) The image processing result of (a).

viation values (in the unit of pixel) of the  $x$  and the  $y$  image coordinates of the parameters  $b$  and  $c$  of the simulated lines are 0.278, 0.353 and 0.037, 0.267, respectively. These standard deviation values were obtained through 16 observations. The analysis results include too many tables to be illustrated here. Only the conclusions are stated as follows.

- By changing the distance between the camera and the origin of the space coordinate system, it was found that the farther the camera is, the larger the standard deviations of the location parameters are.
- When the distance of the camera is fixed, the accuracy of the orientation or position parameters is found to be in proportional to the magnitude of the camera focal length.

TABLE 1. THE LOCATION RESULTS OF THE CUBE IMAGES. THE SYMBOLS "\*" AND "\$" SPECIFY THE LARGEST AND THE SMALLEST ERROR PERCENTAGES, RESPECTIVELY.

Plane	M	$X_c$ (mm) (256.394)	$Y_c$ (mm) (336.976)	$Z_c$ (mm) (404.058)	$\theta$ ( $^\circ$ ) (-35.684)	$\psi$ ( $^\circ$ ) (26.680)	$\delta$ ( $^\circ$ ) (15.752)
TP	<i>m</i>	262.461	339.219	394.797	-36.185	26.851	15.787
	<i>v</i>	6.067	2.243	-9.261	-0.501	0.171	0.035
	<i>e</i>	2.37%	0.66%\$	2.29%*	1.40%	0.64%\$	0.22%\$
	$\sigma$	6.962	6.738	6.013	0.329	0.974	0.539
RP	<i>m</i>	243.768	331.927	407.818	-35.402	25.772	15.060
	<i>v</i>	-12.626	-5.049	3.760	0.282	-0.908	-0.692
	<i>e</i>	4.92%*	1.50%	0.93%	0.79%\$	3.40%	4.39%
	$\sigma$	6.464	5.117	3.659	0.693	0.520	0.693
LP	<i>m</i>	259.985	342.346	406.052	-35.285	27.261	15.906
	<i>v</i>	3.591	5.370	1.962	0.399	0.581	0.154
	<i>e</i>	1.40%\$	1.59%	0.48%	1.11%	2.18%	0.97%
	$\sigma$	9.695	6.195	2.948	0.513	0.371	0.055
PRP	<i>m</i>	245.035	324.702	405.428	-35.002	25.185	15.004
	<i>v</i>	-11.359	-12.274	1.370	0.682	-1.495	-0.748
	<i>e</i>	4.43%	3.64%*	0.34%\$	1.91%*	5.60%*	4.75%*
	$\sigma$	10.223	10.960	2.323	1.074	0.697	0.339

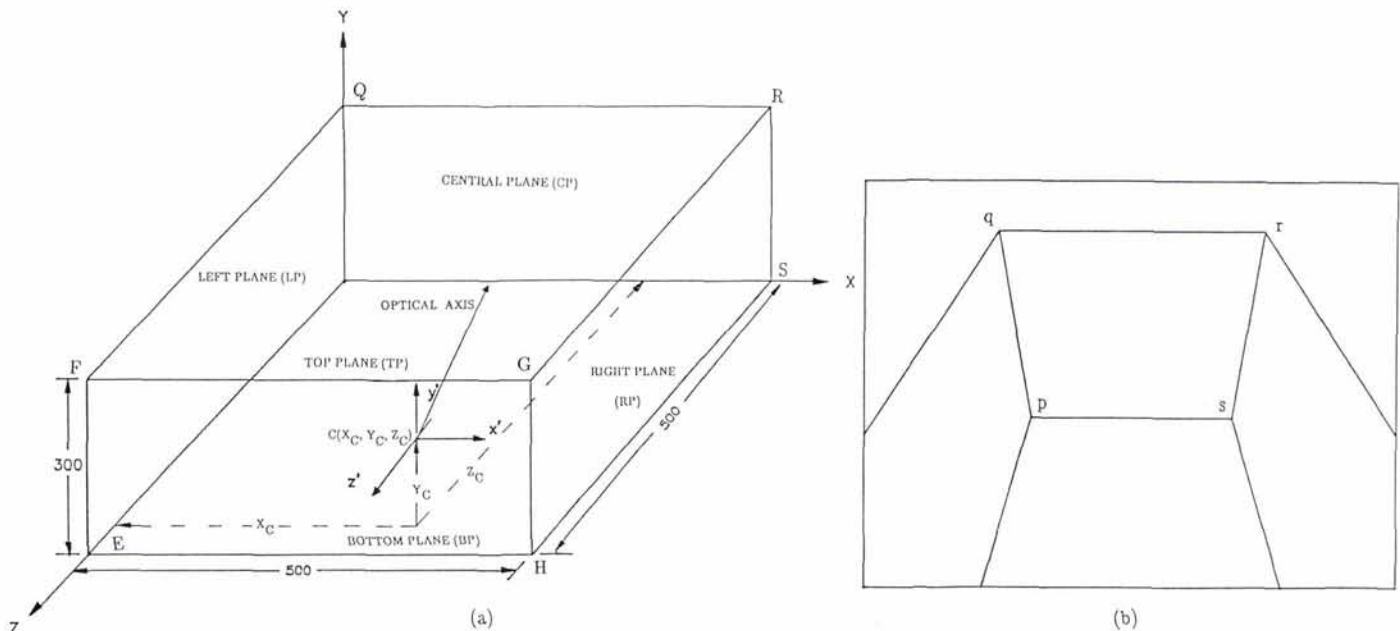


FIG. 7. Robot location in a corridor. (a) The corridor. (b) A simulated corridor image.

- The accuracy of the orientation or position parameters is found to be higher when the side lengths of the rectangular shape are larger.
- To simulate a robot navigating in a corridor like the one shown in Figure 7(a), which consists of four partial planes (namely, the partial left plane (PLP), the partial right plane (PRP), the partial bottom plane (PBP), and the partial top plane (PTP)) and a complete plane (the central plane(CP)), an artificial image of the corridor is created as shown in Figure 7(b). The robot location results using the artificial images are shown in Table 2. The row "T" specifies the weighted average of the location parameters of the above five planes. The central plane yields lower location accuracy than other planes as can be seen from Table 2 because the central plane is the farthest one from the camera.

The computation time for a single rectangular shape using the algebraic formulae of the proposed approach has also been estimated. The estimation is based on the use of a Sun workstation with a fast floating-point arithmetic accelerator requiring 4, 7, 13, 36, 30, and 46  $\mu$ s for addition, multiplication, division,

square root, sine, and tangent function computation, respectively. For a total of 63 additions, 72 multiplications, 9 divisions, 2 square roots, 1 sine function, and 2 tangent functions required for computing the formulae for a single rectangular shape, the computation time is about 1.07 ms, which is approximately 3 percent of the picture grabbing time (1/30 second). But the amounts of image processing time estimated for processing a single rectangular shape are 4, 3, 8, 14, and 3 seconds for edge detection, smoothing, thinning, Hough transformation, and corner point computation, respectively. A total of about 32 seconds is required. This seems too slow. The speed can be improved using parallel processing techniques in the future.

#### CONCLUSIONS AND SUGGESTIONS

A practical approach to robot location has been proposed in this paper. Commonly seen rectangular shapes are taken as the control mark for the location purpose. Algebraic formulae for

TABLE 2. THE LOCATION OF THE SIMULATED IMAGES OF THE CORRIDOR SCENE SHOWN IN FIGURE 7. THE SYMBOLS "\*" AND "\$" SPECIFY THE LARGEST AND THE SMALLEST ERROR PERCENTAGES, RESPECTIVELY.

Plane	S	Xc (mm) (283.109)	Yc (mm) (120.000)	Zc (mm) (416.721)	$\theta$ ( $^{\circ}$ ) (-5.019)	$\psi$ ( $^{\circ}$ ) (4.980)	$\delta$ ( $^{\circ}$ ) (0.437)
PLP	m	283.325	120.114	416.568	-5.012	5.008	0.434
	v	0.216	0.114	-0.153	0.007	0.028	-0.003
	e	0.76%	0.95%*	0.36%*	0.14%*	0.56%*	0.68%
	$\sigma$	0.1346	0.0480	0.0535	0.029	0.115	0.011
PRP	m	283.276	120.015	416.775	-5.023	5.001	0.442
	v	0.167	0.015	0.015	-0.004	0.021	0.005
	e	0.58%	0.12%\$	0.12%	0.08%	0.42%	1.14%
	$\sigma$	0.0997	0.0295	0.0326	0.014	0.087	0.021
CP	m	283.530	120.049	416.707	-5.022	4.985	0.438
	v	0.421	0.049	-0.014	-0.003	0.005	0.001
	e	1.48%*	0.41%	0.03%	0.06%	0.10%	0.22%\$
	$\sigma$	0.1346	0.2005	0.1024	0.011	0.021	0.004
PBP	m	283.114	119.973	416.731	-5.013	4.981	0.431
	v	0.005	-0.027	0.010	0.006	0.001	-0.006
	e	0.02%\$	0.22%	0.02%\$	0.12%	0.02%\$	1.37%*
	$\sigma$	0.0062	0.0038	0.0002	0.021	0.005	0.025
PTP	m	283.246	120.024	416.734	-5.019	4.993	0.442
	v	0.137	0.024	0.013	0.000	0.013	0.005
	e	0.48%	0.20%	0.03%	0.01%\$	0.26%	1.14%
	$\sigma$	0.0017	0.0017	0.0014	0.001	0.053	0.021
T	m	283.150	120.012	416.710	-5.022	4.983	0.437
	v	0.041	0.012	-0.011	-0.003	0.004	0.000
	e	0.014%	0.011%	0.003%	0.003%	0.08%	0.10%
	$\sigma$	0.1070	0.1040	0.0600	0.0197	0.078	0.0204

location determination can be derived easily without linearization. Another advantage of the approach is the ability to use multiple or partial rectangular shapes to compute robot parameters. The location error percentage is less than 5 percent, which shows that the approach is feasible for mobile robot location.

Using better imaging devices, performing more accurate focal length calibrations, and employing subpixel preprocessing techniques (Mikhail *et al.*, 1984) are possible methods to upgrade robot location accuracy. Further research may be directed to extending the location approach to outdoor applications, to applying the proposed approach to mobile robot guidance, to determining robot location using planar curves on a model object surface, and to constructing special purpose hardware for fast location, etc.

#### REFERENCES

- Ackermann, F., 1976. *Photogrammetric*, B. G. Teubner, Stuttgart, West Germany.
- Chen, R. K., Y. T. Tsay, and W. H. Tsai, 1987. 3-D object surface data acquisition using range data, *Proceedings of 1987 Workshop on Computer Vision, Graphics, and Image Processing*, Nantou, Taiwan, Republic of China.
- Chen, Y. S. and W. H. Hsu, 1985. A new parallel thinning algorithm for binary image, *Proceedings of National Computer Symposium*, Kaohsiung, Taiwan, R. O. C.
- Chou, H. L., and W. H. Tsai, 1986. A new approach to robot location by house corners, *Pattern Recognition*, Vol. 19, pp. 439-451.
- Courtney, J. W., and J. K. Aggarwal, 1984. Robot guidance using computer vision, *Pattern Recognition*, Vol. 17, pp. 585-592.
- Duda, R. O., and P. E. Hart, 1972. Use of the Hough transformation to detect lines and curves in pictures, *Commun. ACM*, Vol. 15, pp. 11-15.
- Dudani, S. A., and A. S. Luk, 1978. Locating straight-line edge segments on outdoor scenes, *Pattern Recognition*, Vol. 10, pp. 145-157.
- El-Hakim, S. F., 1984. A photogrammetric vision system for robots, *Proceedings of International Society for Photogrammetry and Remote Sensing, Commission III, Symposium*, pp. 223-231.
- Ethrog, Uzi, 1984. Non-metric camera calibration and photo orientation using parallel and perpendicular lines of the photographed objects, *Photogrammetria*, Vol. 39, pp. 13-22.
- Fukui, I., 1981. TV image processing to determine the position of a robot vehicle, *Pattern Recognition*, Vol. 14, pp. 101-109.
- Haralick, R. M., and Y. H. Chu, 1984. Solving camera from the perspective projection of a parameterized curve, *Pattern Recognition*, Vol. 17, pp. 637-645.
- Horaud, R., 1987. New methods for matching 3-D objects with single perspective views, *IEEE Trans. PAMI*, Vol. PAMI-9, No. 2, pp. 401-412.
- Kratky, V., 1979. Real-time photogrammetric support of dynamic three-dimensional control, *Photogrammetric Engineering and Remote Sensing*, Vol. 45, No. 9, pp. 1231-1242.
- Magee, M. J., and J. K. Aggarwal, 1984. Determining the position of a robot using a single calibration object, *IEEE Conf. on Robotics*, Atlanta, Georgia, pp. 140-149.
- Mikhail, E. M., M. L. Akey, and O. R. Mitchell, 1984. Detection and sub-pixel location of photogrammetric target in digital images, *Photogrammetria*, Vol. 39, pp. 63-83.
- Tommaselli, A. M. G., and J. B. Lugnoni, 1988. An alternative mathematical model to the collinearity equation using straight features, *Proceedings of International Society for Photogrammetry and Remote Sensing, Commission III, Symposium*, pp. 765-774.
- Tsai, R. Y., 1987. A versatile camera calibration technique for high-accuracy 3D machine vision metrology using off-the-shelf TV cameras and lenses, *IEEE Journal of Robotics and Automation*, Vol. RA-3, No. 4, pp. 323-343.
- Tseng, D. C., C. I. Lin, and Z. Chen, 1987. Determining the position of a robot from a single view of a cube., *Proceedings of the 1987 Workshop on Computer Vision, Graphics and Image Processing*, Nantou, Taiwan, Republic of China.
- Wolf, P. R., 1983. *Elements of Photogrammetry*, McGraw-Hill Book Company, Inc., New York, New York, pp. 518-547.
- Wong, K. W., and W. H. Ho, 1986. Close-range mapping with a solid-state camera, *Photogrammetric Engineering and Remote Sensing*, Vol. 52, No. 1, pp. 67-74.

(Received 6 January 1989; revised and accepted 9 May 1989)